Accepted manuscript: *Acta Cryst.* (2012). B**68**, 528-535
doi:10.1107/S0108768112032053
http://scripts.iucr.org/cgi-bin/paper?S0108768112032053

Topological studies of three related MOFs of Gd(III) and 5-nitroisophthalate

Kate Davies[a], Susan A. Bourne[a]*, Lars Öhrström `[b] and Clive L. Oliver[a]

[a]Centre for Supramolecular Chemistry, Department of Chemistry, University of Cape Town, Rondebosch, Cape Town, 7701, South Africa, and [b]Chemical and Biological Engineering, Physical Chemistry, Chalmers University of Technology, Kemivägen 10, Göteborg, Sweden

Correspondence email: susan.bourne@uct.ac.za

Keywords: metal-organic framework; topological analysis; lanthanide

Synopsis

Three gadolinium/5-nitroisophthalate MOFs prepared under controlled but similar conditions were found to be related topologically through a simple C-C bond rotation.

Abstract

The reaction of 5-nitroisophthalic acid (H_2NIA) with $Gd(NO_3)_3{\cdot}6H_2O$ in DMF afforded three new metal-organic frameworks $[Gd(NIA)_{1.5}(DMF)_2]{\cdot}DMF$ (**I**), $[Gd_2(NIA)_3(DMF)_4]{\cdot}xH_2O$ (**II**), and $[Gd_4(NIA)_6(DMF)_{5.5}(H_2O)_3]{\cdot}4DMF{\cdot}H_2O$ (**III**). These compounds can be prepared through a variety of methods. Compounds **I** and **II** are more reproducibly formed than compound **III**. Network analysis revealed **I** to have a $(4^{12}.6^3)$-**pcu** topology while **II** displays a $(4^2.8^4)(4^2.8^4)$-**pts** topology. Compound **III** was found to present the uncommon 4,5,6T11 topological net, which combines aspects of both the **pcu** and **pts** topologies. The short symbol of this net is $(4^4.6^2)(4^6.6^4)_2(4^8.6^6.8)$.

1. Introduction

Metal-organic frameworks (MOFs) and coordination polymers are formed from building blocks made of metal ions and organic linker molecules. The organic linker molecules, if they have three or more points of extension, act as good directional building blocks. The metal ions often have more than one coordination mode, e.g. tetrahedral vs square planar and four- vs six-coordinated, and it is not always

easy to predict which one will be adopted (Hoskins & Robson, 1990; Rowsell & Yaghi, 2004). It is possible to obtain a wide range of these structures from very simple starting materials (Moulton & Zaworotko, 2001). This allows for many uses including catalysis (Horike *et al.*, 2008; Ma *et al.*, 2009), nonlinear optics (Liu *et al.*, 2007; Zhang *et al.*, 2008), gas storage (Chen *et al.*, 2005; Dincă & Long, 2008; Ma & Zhou, 2010; Park & Suh, 2008), sensing (Hallale *et al.*, 2005; Zhang *et al.*, 2010), and luminescence (Black *et al.*, 2009; Che *et al.*, 2008; Yan *et al.*, 2009).

Secondary-building units (SBUs) are conceptual building elements used in the retrosynthetic analysis of MOFs. They can be thought of as formed *in situ* through a self-assembly process (O'Keeffe *et al.*, 2000; Rowsell & Yaghi, 2004), but formally comprise only the bonding modules surrounding the branching points. Often a metal carboxylate polynuclear entity is one SBU (eg. The $(COO)_6Zn_4O$ of MOF5) and an aromatic carboxylate with coordinating metal ions the other (Zn_2OOC-C_6H_4-$COOZn_2$ in MOF5). The SBUs thus act as connection points and have their own geometry and connectivity. They are generally rigid and the reproducibility of SBU formation under specific reaction conditions make them useful in synthesis planning (Rowsell & Yaghi, 2004; Yaghi *et al.*, 2003).

5-nitroisophthalic acid (H_2NIA) possesses rich coordination modes. H_2NIA molecules coordinate particularly well with lanthanide metal ions to form SBUs of lanthanide metal clusters (Chen *et al.*, 2010). These structures may have additional strength through hydrogen bonds. The nitro group is not usually found to coordinate but acts as a hydrogen bond acceptor and these compounds have been found to possess good chemical and thermal stability (Chen *et al.*, 2010). Isophthalic acid has been found to form structures with interesting properties including fluorescence and nonlinear optics (Zhang *et al.*, 2008). The electron withdrawing nitro group influences the electron density of the molecule as a whole, which can lead to different structures than those observed with isophthalic acid (Li *et al.*, 2005). The carboxylic acid moieties are at an angle of 120° to one another, which is thought to be favourable to form rhombic channels in three-dimensional frameworks (Chen *et al.*, 2010). There are a number of reported coordination polymers and MOFs with H_2NIA (Bhunia *et al.*, 2011; Chen *et al.*, 2008; Li *et al.*, 2005; Luo *et al.*, 2003; Tao *et al.*, 2003; Wang *et al.*, 2011; Ye *et al.*, 2008). Relatively few of these are with lanthanides (Chen *et al.*, 2010; Huang *et al.*, 2009; Ren *et al.*, 2006a; Ren *et al.*, 2006b).

Topological or network analysis is the study of the underlying net of a structure: the connectivity of the building blocks and SBUs (Ockwig, 2005; Öhrström, 2012; Öhrström & Larsson, 2005; Yaghi, 2003;). There are many reasons for studying topology but three main ones are that network analysis offers a mental image of the three-dimensional arrangement of the structure, a better understanding of

why certain building blocks form specific structures, and the ability to engineer future structures through a better knowledge of connectivity (Öhrström & Larsson, 2005; O'Keeffe 2009). This paper presents three new, stable MOFs prepared from 5-nitroisophthalic acid and gadolinium(III) nitrate hexahydrate. All three compounds were prepared using multiple methods and the compound formed depended strongly on the method. All three compounds were formed using a 1:1, metal to ligand ratio and slow cooling from elevated temperatures. Compound **I** was formed by immediately allowing the sample to cool to room temperature. The methods used to form compounds **II** and **III** involved the samples being held at elevated temperatures for 24 hours before being cooled to room temperature. Compound **II** tended to form in more concentrated solutions, while less concentrated solutions produced crystals of compound **III**. While two of the new MOFs crystallise with often observed network structures (**pcu** and **pts**), the third formed the relatively new 4,5,6T11 topological net first described by Alexandrov in 2011 (Alexandrov *et al*, 2011). This net contains nodes observed in both the **pcu** and **pts** networks.

2. Experimental

2.1. Materials

Gadolinium(III) nitrate hexahydrate (99.9% purity) was purchased from Sigma Aldrich (Germany) and 5-nitroisophthalic acid (H_2NIA) (>98% purity) was obtained from EGA-Chemie (Germany). Both starting materials were used without further purification.

2.2. Hot-Stage Microscopy

Visual changes on heating were studied using a Nikon SMZ-10 stereoscopic microscope fitted with a Sony Digital Hyper HAD colour video camera. This was connected to a Linkam THMS600 hot stage and a Linkam TP92 controlling unit. Samples were heated at 10 K.min^{-1} and thermal events were captured in realtime.

2.3. Thermogravimetric analysis (TGA)

Compounds were subjected to TGA with a heating rate of 10 K.min^{-1}. Samples were dried on filter paper and placed in an open aluminium crucible. Samples ranged in mass from 5 – 20 mg. A TA-

Accepted manuscript: *Acta Cryst.* (2012). B**68**, 528-535
doi:10.1107/S0108768112032053
http://scripts.iucr.org/cgi-bin/paper?S0108768112032053

Q500 Thermogravimetric Analyser from TA instruments was used with a 50 ml.min^{-1} purging gas flow of dry N_2. TGA traces are provided in the supplementary material.[1]

2.4. Differential Scanning Calorimetry (DSC)

DSC was performed to determine the onset temperatures of guest loss and decomposition. Samples were dried on filter paper and ranged in mass between 1 and 2 mg. They were placed in crimped, vented aluminium pans and were heated at 10 K.min^{-1}. Experiments were performed using a TA instruments DSC-Q200 machine under a dry N_2 atmosphere at 50 mL.min^{-1}. DSC traces are available in the supplementary material.

2.5. X-ray diffraction (XRD)

Compounds **I** and **II** were analysed with powder X-ray diffraction (PXRD). PXRD was used to confirm that the single crystal structure was representative of the bulk material. Due to poor diffraction quality and because it was difficult to produce a sufficient amount of sample, PXRD analysis was not used to study compound **III**. Samples were mounted on a Huber D-83253 Imaging Plate appliance fitted with a Guinier Camera 670, a Huber MC 9300 power supply unit and a Philips PW1120/00 X-ray generator. The generator was fitted with a Huber long fine-focus PW2273/20 tube and a Huber Guinier Monochromator Series 611/15. The samples were exposed to CuKα_1 radiation (λ = 1.5406 Å) produced at 20 mA and 40 kV. The relevant PXRD traces are provided in the supplementary material.

Compounds **I**, **II**, and **III** formed clusters of single crystals and were therefore cut to isolate a monocrystaline fragment of suitable size for data collection. A Nonius Kappa CCD single crystal X-ray diffractometer was used for compounds **I** and **II**. This utilised MoKα radiation (λ = 0.71069 Å) produced at 54 kV and 23 mA with a Nonius FR590 generator. A Bruker KAPPA APEX II DUO single crystal X-ray diffractometer was used for compound **III**. This utilited MoKα radiation

[1] Supplementary data for this paper are available from the IUCr electronic archives (Reference: HW5022). Services for accessing these data are described at the back of the journal.

produced at 50 kV and 30 mA with a Bruker K780 generator. Full crystallographic data are provided in Table 1 and the single crystal data are accessible in the supplementary material.

2.6. Network analysis

Topological analyses were performed by eye and confirmed using the computer programs SYSTRE (Friedrichs 2007), OLEX (Dolomanov *et al.*, 2003), and TOPOS(Blatov 2009; Blatov & Peskov, 2006). These were checked against the Reticular Chemistry Structural Resource (RCSR) (O'Keeffe *et al.*, 2008; O'Keeffe *et al.*, 2009) and EPINET (Ramsden *et al.*, 2009) databases. Compounds **I** and **II** were found to display the **pcu** and **pts** nets respectively. Compound **III** was found to have the 4,5,6T11 topology, observed in comparatively few structures so far. The complete short and long symbols for the three nets are $(4^{12}.6^3)$ and 4·4·4·4·4·4·4·4·4·4·4·4·*·*·* for compound **I**, $(4^2.8^4)(4^2.8^4)$ and $4{\cdot}4{\cdot}8_2{\cdot}8_2{\cdot}8_8{\cdot}8_8$, $4{\cdot}4{\cdot}8_7{\cdot}8_7{\cdot}8_7{\cdot}8_7$ for compound **II**, and $(4^4.6^2)(4^6.6^4)_2(4^8.6^6.8)$ and 4·4·4·4·*·*, $4{\cdot}4{\cdot}4{\cdot}4{\cdot}4{\cdot}4{\cdot}6_2{\cdot}6_2{\cdot}*{\cdot}*$, $4{\cdot}4{\cdot}4{\cdot}4{\cdot}4{\cdot}4{\cdot}4{\cdot}4{\cdot}6_2{\cdot}6_2{\cdot}6_2{\cdot}6_2{\cdot}8_8{\cdot}*{\cdot}*$, for compound **III**. The CD10 values are 1561.0, 977.0 and 1361.50 for compounds **I**, **II**, and **III** respectively.

2.7. Preparation

2.7.1. $[Gd(NIA)_{1.5}(DMF)_2]\cdot DMF$ (I)

86 mg (0.190 mmol) of gadolinium(III) nitrate hexahydrate was dissolved in 1 ml *N*,*N*-dimethylformamide (DMF) and 40 mg (0.189 mmol) of H_2NIA was dissolved in 1 ml DMF, both with heating and stirring. The two solutions were combined, and the vial sealed. The vial was then placed in a Dewar containing water at a temperature of 343 K and allowed to cool slowly to room temperature. Small, pale yellow crystal clusters were obtained with cooling. The single crystal structure reveals two coordinated and one guest DMF molecule in the asymmetric unit. TG and DSC analyses confirm the presence of three DMF molecules in the compound. Found: %C, 35.26; %H, 4.03; %N, 9.02. $C_{21}H_{25.5}GdN_{4.5}O_{12}$ requires %C, 35.83; %H, 3.39; %N, 8.57. Decomp. > 603 K.

2.7.2. $[Gd_2(NIA)_3(DMF)_4]\cdot xH_2O$ (II)

86 mg (0.190 mmol) of gadolinium(III) nitrate hexahydrate was dissolved in 1 ml DMF with heating and stirring. 40 mg (0.189 mmol) of NIA was dissolved in 1 ml DMF with heating and stirring. The two solutions were combined and the vial sealed. The vial was then placed in an oil bath at 333 K and held at that temperature for 24 hours. The oil bath was cooled to room temperature over 48 hours

(0.83 K/hour). Small, pale yellow crystal clusters were obtained with cooling. 2.7 guest water molecules were modelled in the single crystal structure. The structure reveals that the guest water molecules are located in pockets in the framework. The water content of these pockets is fixed upon crystallisation and varies from crystal to crystal as elaborated in greater detail in Section 3.2. As a result the TG trace shows the loss of only 1.9 water molecules while the elemental analysis shows a good fit with 1.5 water molecules present. Found: %C, 34.54; %H, 3.94; %N, 8.33. $C_{36}H_{37}Gd_2N_7O_{22}\cdot 1.5H_2O$ requires %C, 34.28; %H, 3.20; %N, 7.77. Decomp. > 603 K.

2.7.3. $[Gd_4(NIA)_6(DMF)_{5.5}(H_2O)_3]\cdot 4DMF\cdot H_2O$

43 mg (0.0953 mmol) of gadolinium(III) nitrate hexahydrate was dissolved in 1 ml DMF and 20 mg (0.0947 mmol) of NIA was dissolved in 1 ml DMF, both with heating and stirring. The two solutions were combined and the vial sealed. The vial was then placed in an oil bath at 333 K and held at that temperature for 24 hours. The oil bath was cooled to room temperature over 48 hours (0.83 K/hour). Small, pale yellow crystal clusters were obtained with cooling. The single crystal structure reveals four guest and three coordinated DMF molecules as well as one guest and three coordinated water molecules. TG and DSC analyses confirm the presence of the guest molecules. HSM shows that decomposition starts as the coordinated DMF and water molecules begin to be removed. The compound also loses the guest DMF at relatively low temperatures, and is capable of absorbing water from the atmosphere. Therefore the elemental analysis reported corresponds to the loss of a guest DMF molecule from the sample and the absorption of two additional water molecules. Found: %C, 33.41; %H, 3.84; %N, 8.04. $C_{73.5}H_{89.5}Gd_4N_{14.5}O_{50.5}$ requires %C, 33.78; %H, 3.45; %N, 7.77. Decomp. *ca* 413 K.

All three compounds were obtained with varying metal to ligand ratios and could be grown at a temperature of 353 K although single crystal quality was poorer. Compound **III** could not be studied with PXRD analysis due to the poor diffraction quality of the powder. Amorphous material and starting materials were often obtained in vials containing crystals of compound **III**. **III** was not obtained as reliably as compounds **I** and **II**.

3. Results and Discussion

Accepted manuscript: *Acta Cryst.* (2012). B**68**, 528-535
doi:10.1107/S0108768112032053
http://scripts.iucr.org/cgi-bin/paper?S0108768112032053

3.1. $[Gd(NIA)_{1.5}(DMF)_2]\cdot DMF$ (I)

Figure 1 shows the asymmetric unit of **I** with hydrogen atoms excluded for clarity. The asymmetric unit consists of one metal centre, one and a half 5-nitroisophthalate ligands, two coordinated DMF molecules, and one guest DMF molecule. The Gd1 metal ion is coordinated to eight oxygen atoms in a distorted square, antiprismatic manner. A Gd1 metal dimer acts as a secondary-building unit (SBU) as shown in Figure 2. This SBU (A) comprises four fully deprotonated NIA units bridging the two Gd1 metal centres in a paddle-wheel fashion. A further NIA unit is bound in a bidentate fashion through one carboxylate moiety to each metal centre. There are also two DMF molecules (not shown) coordinated to each metal ion. Each NIA unit acts as a connector to another SBU. Network analysis of compound **I** reveals the **pcu** network (Figure 3). This net is uninodal with the six-connected nodes placed between the two metal centres of the paddle-wheel motif. These nodes are connected in a distorted octahedral fashion.

I forms a three-dimensional framework with channels along the [010] direction. There are six isostructural compounds (Chen *et al.*, 2010; Wang *et al.*, 2010) reported in the Cambridge Structural Database (CSD, February 2011). Compound **I** was prepared under significantly different conditions however, and required no templating material. There are five mass loss steps observed in the TG trace (A, B, C, D, and E), which correlate with the endotherms observed in the DSC trace. The steps A – D are close together and correspond to the loss of the two coordinated and one guest DMF molecule. The loss of the final DMF molecules ends at approximately 608 K and almost directly after this temperature decomposition begins (mass loss E). Hot-stage microscopy shows that the crystal begins to become opaque with the loss of half a DMF molecule. After the loss of 1.5 DMF molecules (423 K) the crystal is completely opaque and variable temperature PXRD experiments confirm that this corresponds with a decrease in crystallinity. The sample is almost completely amorphous by 473 K. Discolouration due to decomposition is only observed in HSM after 573 K.

A sample of **I** was heated at 383 K for approximately 30 hours and TG analysis revealed a mass loss corresponding to the loss of two of the three modelled DMF molecules. This partially desolvated sample was exposed to DMF vapour for 36 hours and TG analysis showed that one DMF molecule had been reabsorbed (two DMF molecules were removed from the structure with heating to 598 K). There are some additional peaks in the PXRD trace of the partially resolvated sample compared to the trace for compound **I**, but the overall pattern is very similar to that found for **I**.

Accepted manuscript: *Acta Cryst.* (2012). B**68**, 528-535
doi:10.1107/S0108768112032053
http://scripts.iucr.org/cgi-bin/paper?S0108768112032053

3.2. $[Gd_2(NIA)_3(DMF)_4]\cdot xH_2O$ (II)

Figure 4 shows the asymmetric unit of **II** with the hydrogen atoms and guest water molecules omitted. The oxygen atoms of the DMF molecules coordinated to each metal centre are shown. The asymmetric unit consists of two metal centres, three fully deprotonated NIA anions, four coordinated DMF molecules and 2.7 guest water molecules disordered over 6 positions. One of the NIA units (1) bridges metal centres with both carboxylate moieties while the other two NIA units (2 and 3) bridge metal centres with one carboxylate and are chelated through the other carboxylate to a single metal ion. Each gadolinium metal ion is coordinated to eight oxygen atoms in a distorted square, antiprismatic fashion similar to that observed for compound **I**. A Gd1 metal dimer acts as one SBU (B) (Figure 5a) while a Gd2 metal dimer acts as a second SBU (C) (Figure 5b). Both SBUs consist of four fully deprotonated NIA units bridging the two metal centres in a paddle-wheel fashion, a further NIA unit doubly coordinated to each metal centre, and two DMF molecules coordinated to each metal centre. SBUs B and C appear similar to SBU A when coordination around the metal centres is observed. However, in compound **I** each NIA unit of SBU A connects to a another SBU A. In compound **II** for every NIA 2 spanning two SBU there is an NIA 3 spanning the same two SBU, while each NIA 1 connects to a different SBU (Figure 5). As a result the connectivity of SBUs B and C is 4-connected rather than the 6-connected node seen in SBU A. Topological analysis of compound **II** reveals the **pts** network (Figure 6). This net is bidnodal with both of the four-connected nodes placed between two metal centres of a paddle-wheel motif. The node in SBU B connects in a distorted square-planar manner while the node in SBU C connects in a distorted tetrahedral manner.

II forms a three-dimensional framework with the guest water molecules located in “pockets” formed by the framework. There are no channels within the framework implying that the water present in these pockets is trapped upon complexation. The SQUEEZE routine in PLATON (Spek, 2003) indicates no residual electron density, thus implying that all the water molecules present were modelled. With the guest water molecules deleted from the structure *ca* 2125.8 $Å^3$ solvent accessible void space was observed, equating to space for *ca* 6.5 water molecules per asymmetric unit. The discrepancy (2.7 modelled water molecules versus space for 6.5 in the empty framework) is accounted for by the disorder of the modelled water molecules. This void space implies that the water content can vary from crystal to crystal. The residual electron density confirmed that no additional water molecules could be modelled for the crystal selected for analysis.

Accepted manuscript: *Acta Cryst.* (2012). B**68**, 528-535
doi:10.1107/S0108768112032053
http://scripts.iucr.org/cgi-bin/paper?S0108768112032053

There are three mass loss steps (A, B, and C) visible in the TG trace. Mass loss A corresponds to the loss of 1.9 water molecules, which further confirms that the water content in compound **II** is variable from crystal to crystal. Mass loss B corresponds to the loss of the four coordinated DMF molecules. Decomposition begins immediately after the loss of the final DMF molecule. Mass loss C corresponds to complete decomposition. The DSC trace correlates well with the TG analysis. HSM analysis reveals that compound **II** begins to lose single crystallinity immediately with the removal of the guest water molecules, it becomes completely opaque at approximately 430 K and remains so until all the DMF molecules have been removed. After this the crystal starts to discolour corresponding with the beginning of decomposition.

3.3. Comparison between I and II

Rotation around the C6-C7 bond of one NIA unit of **I** (see Figure 7a) would allow O1 of the O1-C1-O2 carboxylate moiety to coordinate to the same metal centre as O5 and O6 of the O5-C7-O6 carboxylate moiety on the adjacent NIA unit. The relevant NIA units are highlighted in blue in the figure. In compound **II** this rotation has occurred as shown in Figure 7b. Again the pertinent NIA units are highlighted in blue. O12 of the O11-C15-O12 carboxylate and both O17 and O18 of the O17-C23-O18 carboxylate are coordinated to the Gd2 metal centre in compound **II**. The result of this is that the six-connected node found in compound **I** is no longer present in compound **II**. Instead four-connected nodes are found.

3.4. $[Gd_4(NIA)_6(DMF)_{5.5}(H_2O)_3]\cdot 4DMF\cdot H_2O$ (III)

Figure 8 shows the asymmetric unit of **III** with hydrogen atoms, guest water molecules and guest DMF molecules omitted. The oxygen atoms of the coordinated DMF molecules are shown. The asymmetric unit consists of four metal centres, six 5-nitroisophthalate ligands, five and a half coordinated DMF molecules, four guest DMF molecules, three coordinated water molecules, and one guest water molecule. The Gd1, Gd2, and Gd3 metal ions are each coordinated to eight oxygen atoms in a distorted square, antiprismatic manner. Figure 9 shows that Gd1 forms a dimer with another Gd1 metal centre and the resulting SBU D consists of four NIA units that bridge the metal ions, a further NIA unit chelated to each metal centre, and two DMF molecules coordinated to each metal ion. SBU D is similar to SBU A (compound **I**) forming a 6-connected, distorted octahedral node. Gd2 and Gd3 form a dimer and the resulting SBU E consists of four NIA units that bridge the metal ion. Another

Accepted manuscript: *Acta Cryst.* (2012). B**68**, 528-535
doi:10.1107/S0108768112032053
http://scripts.iucr.org/cgi-bin/paper?S0108768112032053

NIA unit is coordinated in a bidentate fashion to the Gd2 metal centre and an NIA unit is coordinated through one oxygen atom to the Gd3 metal centre. Gd2 is also coordinated to two DMF molecules while Gd3 is coordinated to two DMF molecules as well as one water molecule. SBU E is very similar to SBU B for compound **II** in that it forms a 4-connected, distorted square planar node. The Gd4 metal ion is coordinated to seven oxygen atoms. Four oxygen atoms are from NIA units that bridge a Gd4/Gd4* metal pair in a paddle-wheel fashion to form SBU F. A further NIA unit is singly coordinated to each metal ion as well as a DMF molecule and a water molecule. SBU F forms a 5-connected node, which acts as a connector between the 4- and 6-connected nodes. Each 5-connected node contains NIA units where the previously described C-C rotation has occurred (as for **II**) and NIA units where it has not occurred (as for **I**).

Network analysis of compound **III** revealed the 4,5,6T11 trinodal three-dimensional net. The short symbol of this net is $(4^4.6^2)(4^6.6^4)_2(4^8.6^6.8)$. There are two 5-connected nodes for every one 4- and one 6-connected node. A schematic view of the net connectivity is given in Figure 9. This shows that while all the nodes are placed between a pair of Gd metal centres they each have different connectivity. As can be seen in Figure 10 all of the 4- and 6-connected nodes are joined solely to 5-connected nodes. TG analysis of compound **III** reveals four mass loss steps (A, B, C, and D). Step A corresponds to the loss of the guest water molecule and one guest DMF molecule. Step B corresponds to the loss of the other three guest DMF molecules. Step C corresponds to the loss of the 5.5 coordinated DMF molecules and full decomposition (step D) begins as soon as the last DMF is removed. DSC correlates well with TG analysis. HSM reveals that the crystal begins to crack with the loss of the DMF molecules. As the coordinated DMF molecules start to be removed from the structure (approximately 423 K) the sample becomes completely black and with full decomposition (643 K) the crystal fractures.

4. Conclusions

All three compounds reported here are neutral MOFs. Compound **I** is isostructural to six compounds reported in the literature and can be partially desolvated and resolvated with DMF vapour. **I** forms the **pcu**-net and has rhombohedral pores occupied by guest DMF molecules. Compound **II** contains large, enclosed void spaces. The water content of **II** varies from crystal to crystal. **II** forms the **pts**-net and is related to **I** through the rotation around a C-C bond. Compound **III** forms the 4,5,6T11 net, which contains aspects of both the octahedral 6-connected node of **I** and the square-planar 4-connected node of **II**. These 4- and 6-connected nodes are joined by a 5-connected node. The 5-connected SBU

contains both NIA units that have undergone the C-C rotation and those that have not. Topological analysis allowed the underlying similarities and differences between these compounds to be examined more easily.

Acknowledgements Financial support was received from the South African National Research Foundation (Grant CPR20100409000010269). We thank the Swedish Research Council (VR) and the Swedish International Development Agency (SIDA) for a Swedish Research Links planning grant. KD thanks the University of Cape Town (UCT), the UCT Department of Chemistry Equity and Development Program (EDP), and the National Research Foundation for funding.

References

Alexandrov, E. V., Blatov, V. A., Kochetkov, A. V. & Proserpio, D. M. (2011). *CrystEngComm*, 13, 3947-3958.

Bhunia, M. K., Das, S. K., Seikh, M. M., Domasevitch, K. V. & Bhaumik, A. (2011). *Polyhedron*, 30, 2218-2226.

Black, C. A., Costa, J. S., Fu, W. T., Massera, C., Roubeau, O., Teat, S. J., Aromí, G., Gamez, P. & Reedijk, J. (2009). *Inorg. Chem.*, 48, 1062-1068.

Blatov, V. A. (2009). TOPOS 4.0, http://www.topos.ssu.samara.ru/.

Blatov, V. A. & Peskov, M. V. (2006). *Acta Cryst.*, 62, 457-466.

Cambridge Structural Database and Cambridge Structural Database System, Version 5.32, Cambridge Crystallographic Data Centre, University Chemical Laboratory, Cambridge, England, February 2011 .

Che, G. B., Liu, C. B., Liu, B., Wang, Q. W. & Xu, Z. L. (2008). *CrystEngComm*, 10, 184-191.

Chen, B., Ockwig, N. W., Millward, A. R., Contreras, D. S. & Yaghi, O. M. (2005). *Angew. Chem. Int. Ed.*, 44, 4745-4749.

Chen, Q., Yang, E. -C., Zhang, R. -W., Wang, X. -G. & Zhao, X. -J. (2008). *J. Coord. Chem.*, 61, 1951-1962.

Chen, S. -P., Ren, Y. -X., Wang, W. -T. & Gao, S. -L. (2010). *Dalton Trans.*, 39, 1552-1557.

Dincă, M. & Long, J. R. (2008). *Angew. Chem. Int. Ed.*, 47, 6766-6779.

Dolomanov, O. V., Blake, A. J., Champness, N. R. & Schröder, M. (2003). *J. Appl. Cryst.*, 36, 1283-1284.

Friedrichs, O. D. Program SYSTRE 1.14 beta http://gavrog.sourceforge.net/, 2007.

Hallale, O., Bourne, S. A. & Koch, K. R. (2005). *New J. Chem.*, 29, 1416-1423.

Horike, S., Dincă, M., Tamaki, K. & Long, J. R. (2008). *J. Am. Chem. Soc.*, 130, 5854-5855.

Hoskins, B. F. & Robson, R. (1990). *J. Am. Chem. Soc.*, 112, 1546-1554.

Huang, Y., Yan, B. & Shao, M. (2009). *J. Solid State Chem.*, 182, 657-668.

Li, X., Cao, R., Bi, W., Wang, Y., Wang, Y., Li, X. & Guo, Z. (2005). *Cryst. Growth Des.*, 5, 1651-1656.

Liu, Y., Li, G., Li, X. & Cui, Y. (2007). *Angew.Chem.Int.Ed*, 46, 6301-6304.

Luo, J., Hong, M., Wang, R., Cao, R., Han, L., Yuan, D., Lin, Z. & Zhou, Y. (2003). *Inorg. Chem.*, 42, 4486-4488.

Ma, L., Abney, C. & Lin, W. (2009). *Chem. Soc. Rev.*, 38, 1248-1256.

Ma, S. & Zhou, H. C. (2010). *Chem. Commun.*, 46, 44-53.

Moulton, B. & Zaworotko, M. J. (2001). *Chem.Rev.*, 101, 1629-1658.

Ockwig, N. W., Delgado-Friedrichs, O., O'Keeffe, M. & Yaghi, O. M. (2005) *Acc. Chem. Res.,* 38, 176-182.

Öhrström, L. & Larsson, K. (2005). *Molecule-based Materials the Structural Network Approach,* 1st ed. Amsterdam, The Netherlands: Elsevier.

Öhrström, L. (2012). *Supramolecular Chemistry: From Molecules to Nanomaterials,* Vol. 6. Chichester, UK: John Wiley & Sons.

O'Keeffe, M. (2009). *Chem. Soc. Rev.*, 38, 1215-1217.

O'Keeffe, M., Eddaoudi, M., Li, H., Reineke, T. & Yaghi, O. M. (2000). *J. Solid State Chem.*, 152, 3-20.

O'Keeffe, M., Peskov, M. A., Ramsden, S. & Yaghi, O. M. (2008). *Acc. Chem. Res.*, 41, 1782-1789.

O'Keeffe, M., Yaghi, O. M. & Ramsden, S. Australian National University Supercomputer Facility, Reticular Chemistry Structure Resource, http://rcsr.anu.edu.ac/, 2009.

Park, H. J. & Suh, M. P. (2008). *Chem. Eur. J.*, 14, 8812-8821.

Ramsden, S. J., Robins, V., Hungerford, S. & Hyde, S. T. EPINET, http://epinet.anu.adu.au, 2009.

Ren, Y., Chen, S. & Gao, S. (2006a). *J. Coord. Chem.*, 59, 2135-2142.

Ren, Y., Chen, S., Xie, G., Gao, S. & Shi, Q. (2006b). *Inorg. Chim. Acta,* 359, 2047-2052.

Rowsell, J. L. C. & Yaghi, O. M. (2004). *Micropor. Mesopor. Mat.*, 73, 3-14.

Spek, A.L. (2003), *J. Appl. Cryst.*, 36, 7-13.

Tao, J., Yin, X., Jiang, Y. -B., Yang, L. -F., Huang, R. -B. & Zheng, L. -S. (2003). *Eur. J. Inorg. Chem.*, 2678-2682.

Wang, G., Song, T., Fan, Y., Wan, W., Xu, J. & Wang, L. (2010). *Inorg. Chem. Commun.*, 13, 935-937.

Wang, J., Qian, X., Cui, Y. -F., Li, B. -L. & Li, H. -Y. (2011). *J. Coord. Chem.*, 64, 2878-2889.

Yaghi, O. M., O'Keeffe, M., Ockwig, N. W., Chae, H. K., Eddaoudi, M. & Kim, J. (2003). *Nature*, 423, 705-714.

Yan, L., Yue, Q., Jia, Q. -X., Lemercier, G. & Gao, E. -Q. (2009). *Cryst. Growth & Des.*, 9, 2984-2987.

Ye, J., Wang, J., Wu, Y., Ye, L. & Zhang, P. (2008). *J. Mol. Struct.*, 873, 35-40.

Zhang, L., Qin, Y. -Y., Li, Z. -J., Lin, Q. -P., Cheng, J. -K., Zhang, J. & Yao, Y. -G. (2008). *Inorg. Chem.*, 47, 8286-8293.

Zhang, Z., Xiang, S., Rao, X., Zheng, Q., Fronczek, F. R., Qian, G. & Chen, B. (2010). *Chem. Commun.*, 46, 7205-7207.

Accepted manuscript: *Acta Cryst.* (2012). B**68**, 528-535
doi:10.1107/S0108768112032053
http://scripts.iucr.org/cgi-bin/paper?S0108768112032053

Table 1 Crystal data and refinement parameters for $[Gd(NIA)_{1.5}(DMF)_2]\cdot DMF$ (**I**), $[Gd_2(NIA)_3(DMF)_4]\cdot 2.67H_2O$ (**II**), and $[Gd_4(NIA)_6(DMF)_{5.5}(H_2O)_3]\cdot 4DMF\cdot H_2O$ (**III**)

Crystallographic Data	Compound **I**	Compound **II**	Compound **III**
Empirical Formula	$C_{21}H_{25.5}GdN_{4.5}O_{12}$	$C_{36}H_{42.4}Gd_2N_7O_{24.7}$	$C_{76.5}H_{92.5}Gd_4N_{15.5}O_{49.5}$
Formula Weight (g.mol^{-1})	690.21	1282.34	2650.16
Temperature (K)	173(2)	173(2)	173(2)
Wavelength (Å)	0.71073	0.71073	0.71073
Crystal System	Monoclinic	Monoclinic	Triclinic
Space Group	*C*2/*c*	*C*2/*c*	$P\bar{1}$
a (Å)	21.622(4)	24.9427(2)	14.324(2)
b (Å)	16.800(3)	16.9411(2)	15.317(2)
c (Å)	16.317(3)	25.2889(2)	25.468(3)
α (°)	90	90	87.994(2)
β (°)	119.628(4)	105.208(1)	85.151(2)
ɣ (°)	90	90	63.419(2)
Volume (Å^3)	5152(2)	10311.8(2)	4979(1)
Z	8	8	2
D_{calcd} (g.cm^{-3})	1.780	1.652	1.768
Crystal Size (mm)	0.30 x 0.25 x 0.20	0.30 x 0.20 x 0.15	0.43 x 0.28 x 0.18
***Θ*-Range Scanned (°)**	2.82 – 30.51	1.58 – 27.48	1.59 – 28.45
Index Range	$-30 \le h \le 22$, $-23 \le k \le 21$, $-11 \le l \le 23$	$-32 \le h \le 32$, $-21 \le k \le 21$, $-32 < l \le 32$	$-19 \le h \le 19$, $-20 \le k \le 20$, $-34 < l \le 34$
Reflections Collected	32987	180368	190792
Independent Reflections	7835	11826	24969
Restraints	0	0	17
Parameters	355	616	1303
***R*$_{int}$**	0.0225	0.0824	0.0336

Accepted manuscript: *Acta Cryst.* (2012). B**68**, 528-535
doi:10.1107/S0108768112032053
http://scripts.iucr.org/cgi-bin/paper?S0108768112032053

Goodness-of-fit	1.060	1.130	1.127
R_1 **[**$I>2\sigma(I)$**]**	0.0193	0.0402	0.0480
wR_2	0.0484	0.1040	0.1141
***R* Indices (all data)**	$R_1 = 0.0240$, $wR_2 = 0.0506$	$R_1 = 0.0538$, $wR_2 = 0.1139$	$R_1 = 0.0576$, $wR_2 = 0.1216$
Largest Diff. Peak and Hole (*e*.*A*$^{-3}$)	1.194, -0.981	1.732, -2.087	6.049, -2.347

Accepted manuscript: *Acta Cryst.* (2012). B**68**, 528-535
doi:10.1107/S0108768112032053
http://scripts.iucr.org/cgi-bin/paper?S0108768112032053

Figure captions

Figure 1 Compound **I** with the asymmetric unit labelled and the hydrogen atoms omitted for clarity.

Figure 2 The Gd1/Gd1* secondary-building unit (SBU) of compound **I** where four NIA units form the paddle-wheel and a further two NIA units are axially coordinated. The hydrogen atoms and DMF molecules are omitted for clarity.

Figure 3 The topological **pcu** net as seen in compound **I**.

Figure 4 Compound **II** with the asymmetric unit labelled. The hydrogen atoms and guest water molecules are omitted for clarity. Only the oxygen atoms of the coordinated DMF molecules are shown.

Figure 5 The SBUs of compound **II**. **a)** Two NIA 1 and two NIA 3 form the paddle-wheel and two NIA 2 are axially coordinated in SBU B. **b)** Two NIA 1 and two NIA 2 form the paddle-wheel and two NIA 3 are axially coordinated in SBU C. Hydrogen atoms, DMF and guest water molecules are omitted for clarity.

Figure 6 The topological **pts** net as seen in compound **II**.

Figure 7 Paddle-wheel SBU demonstrating the C-C rotation which relates **a) I** to **b) II** with the relevant NIA units given in blue.

Figure 8 Compound **III** with the asymmetric unit labelled. The hydrogen atoms, DMF molecules and guest water molecules are omitted for clarity. The oxygen atoms of the coordinated DMF molecules are shown.

Figure 9 A schematic diagram of the octahedral six-connected node at SBU D (blue), square-planar four-connected node at SBU E (red), and five-connected node at SBU F (green) found in compound **III**.

Figure 10 The topological net of **III** with the 4-connected node in red, the 5-connected node in green and the 6-connected node in blue.

Accepted manuscript: *Acta Cryst.* (2012). B**68**, 528-535
doi:10.1107/S0108768112032053
http://scripts.iucr.org/cgi-bin/paper?S0108768112032053

Accepted manuscript: *Acta Cryst.* (2012). B**68**, 528-535
doi:10.1107/S0108768112032053
http://scripts.iucr.org/cgi-bin/paper?S0108768112032053

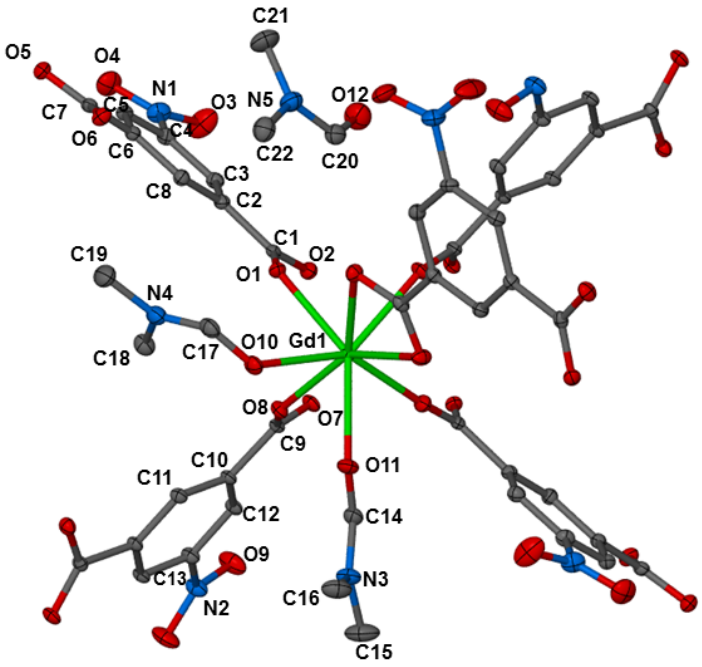

Figure 1

Accepted manuscript: *Acta Cryst.* (2012). B**68**, 528-535
doi:10.1107/S0108768112032053
http://scripts.iucr.org/cgi-bin/paper?S0108768112032053

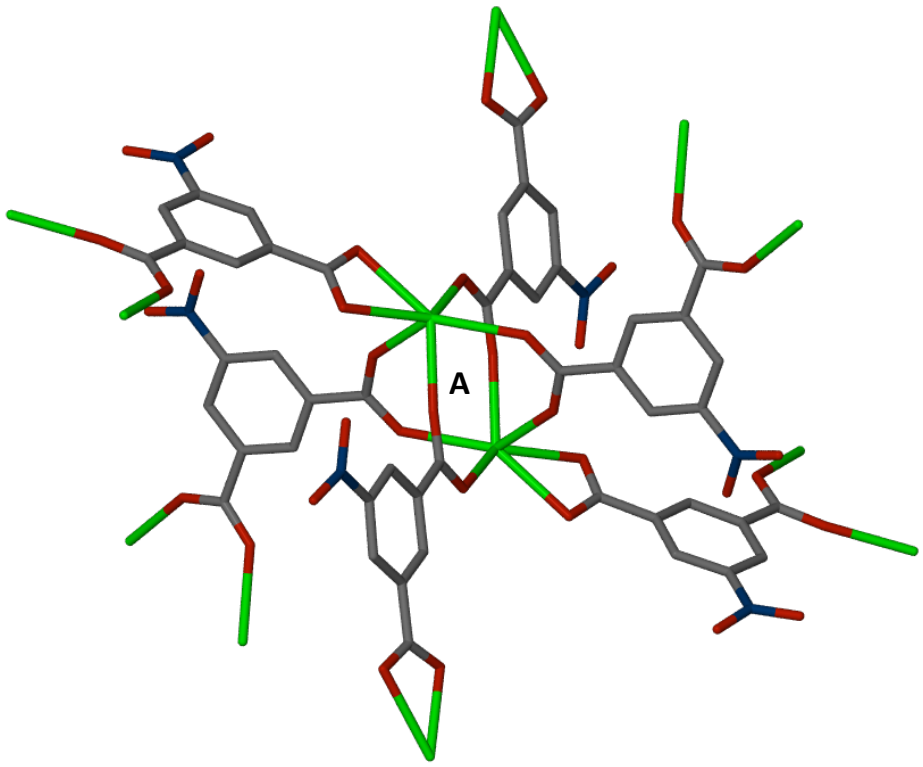

Figure 2

Accepted manuscript: *Acta Cryst.* (2012). B**68**, 528-535
doi:10.1107/S0108768112032053
http://scripts.iucr.org/cgi-bin/paper?S0108768112032053

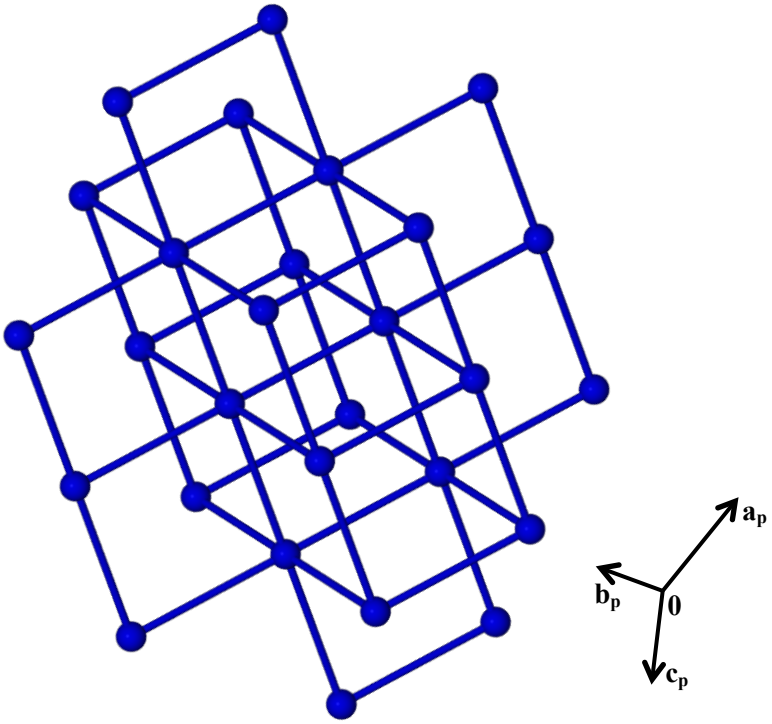

Figure 3

Accepted manuscript: *Acta Cryst.* (2012). B**68**, 528-535
doi:10.1107/S0108768112032053
http://scripts.iucr.org/cgi-bin/paper?S0108768112032053

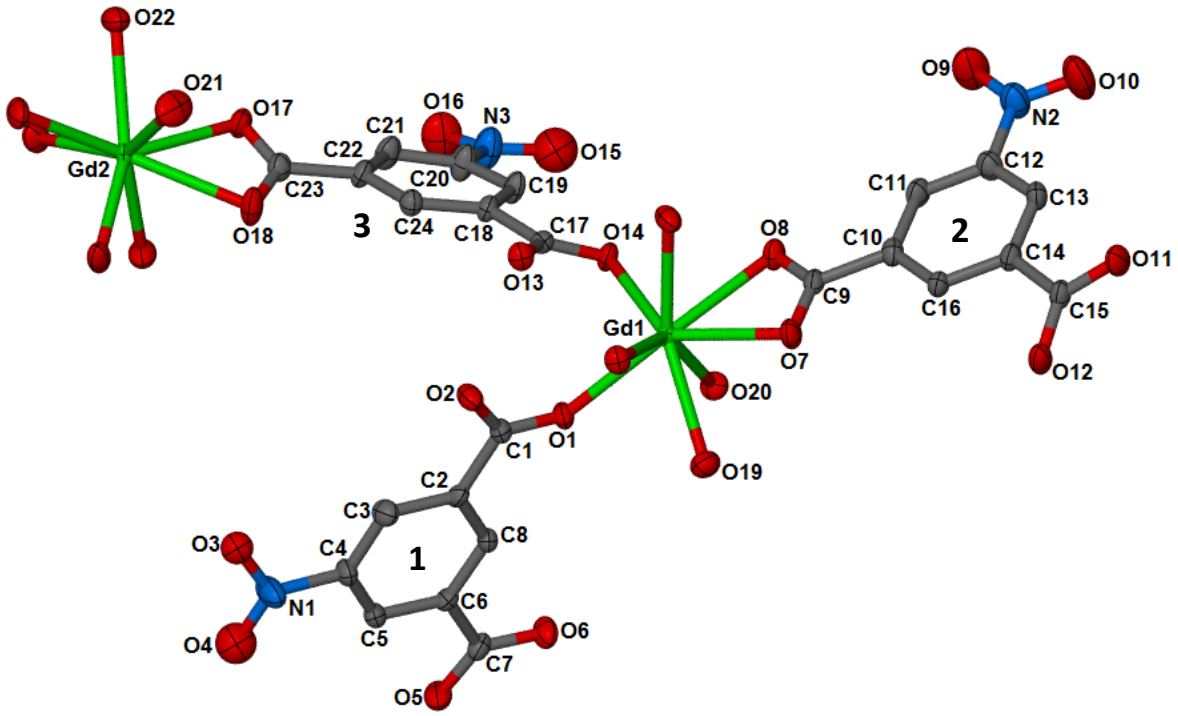

Figure 4

Accepted manuscript: *Acta Cryst.* (2012). B**68**, 528-535
doi:10.1107/S0108768112032053
http://scripts.iucr.org/cgi-bin/paper?S0108768112032053

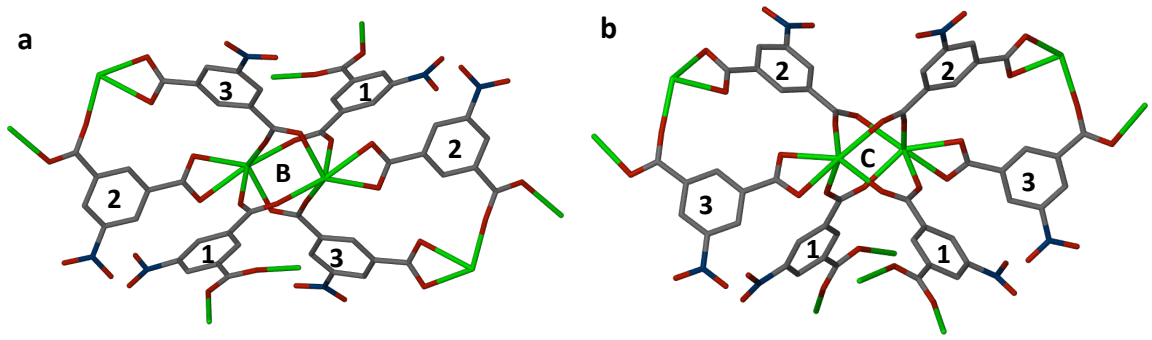

Figure 5

Accepted manuscript: *Acta Cryst.* (2012). B**68**, 528-535
doi:10.1107/S0108768112032053
http://scripts.iucr.org/cgi-bin/paper?S0108768112032053

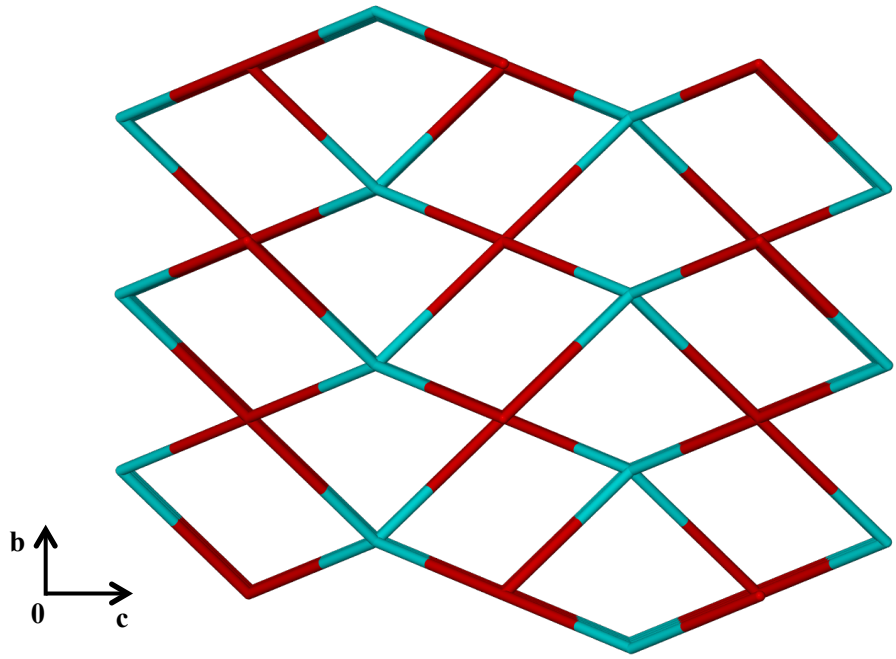

Figure 6

Accepted manuscript: *Acta Cryst.* (2012). B**68**, 528-535
doi:10.1107/S0108768112032053
http://scripts.iucr.org/cgi-bin/paper?S0108768112032053

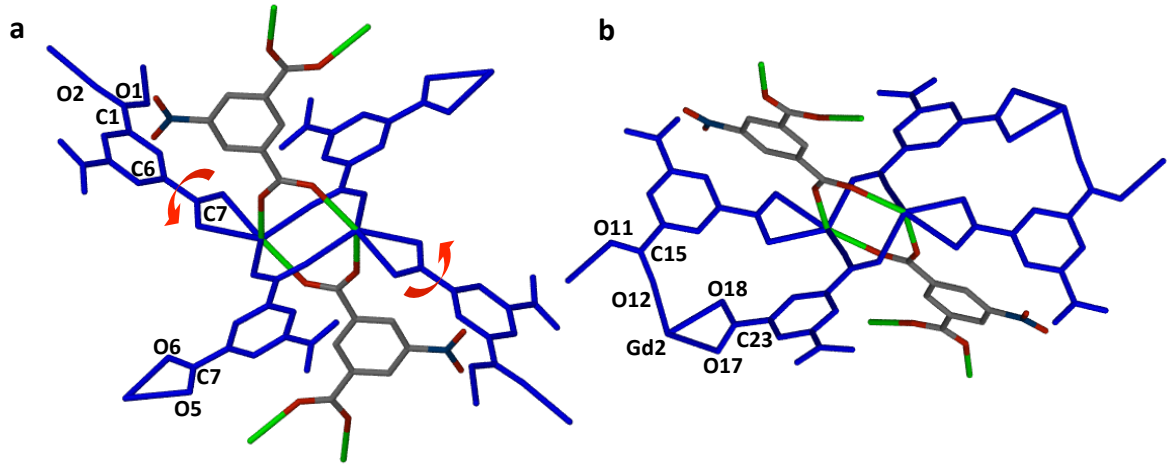

Figure 7

Accepted manuscript: *Acta Cryst.* (2012). B**68**, 528-535
doi:10.1107/S0108768112032053
http://scripts.iucr.org/cgi-bin/paper?S0108768112032053

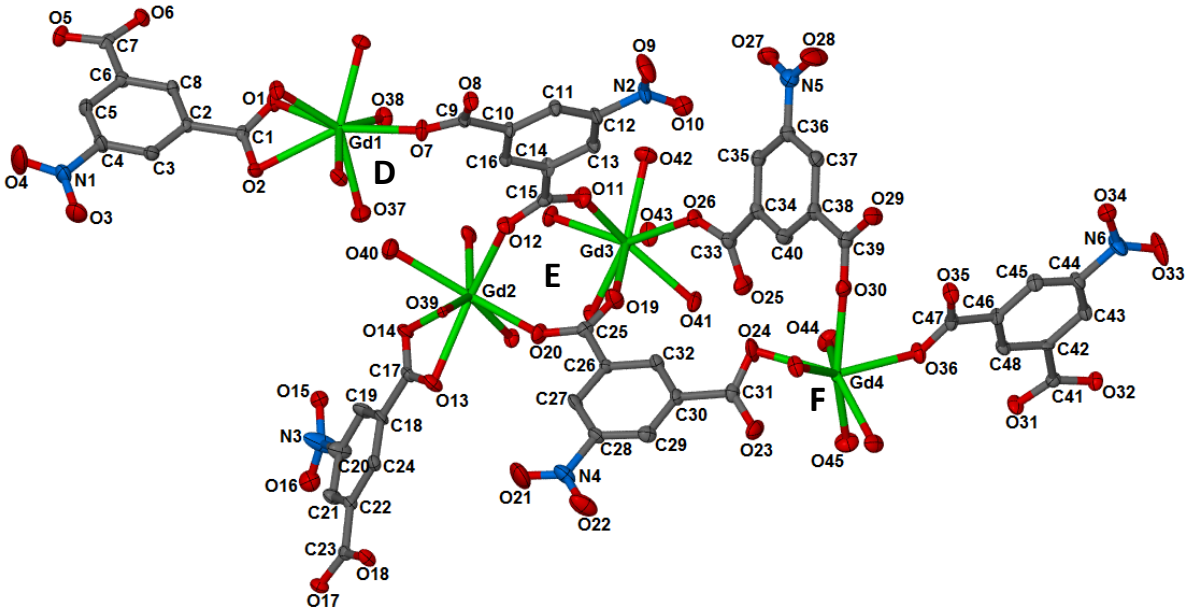

Figure 8

Accepted manuscript: *Acta Cryst.* (2012). B**68**, 528-535
doi:10.1107/S0108768112032053
http://scripts.iucr.org/cgi-bin/paper?S0108768112032053

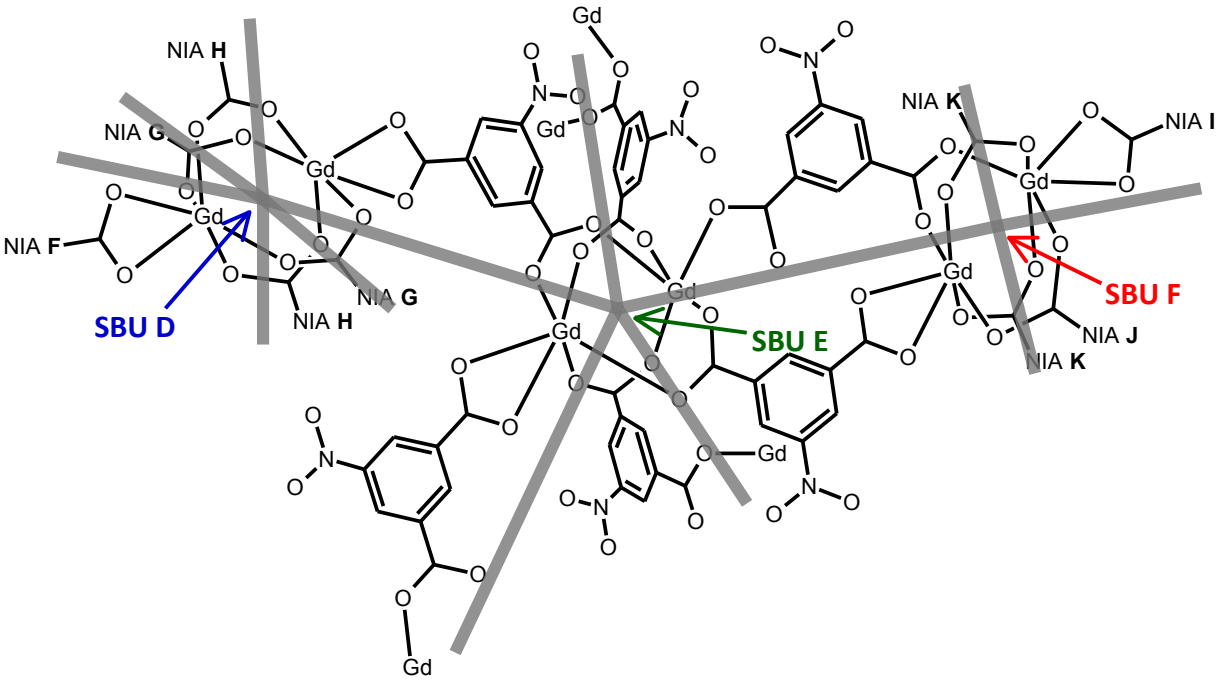

Figure 9

Accepted manuscript: *Acta Cryst.* (2012). B**68**, 528-535
doi:10.1107/S0108768112032053
http://scripts.iucr.org/cgi-bin/paper?S0108768112032053

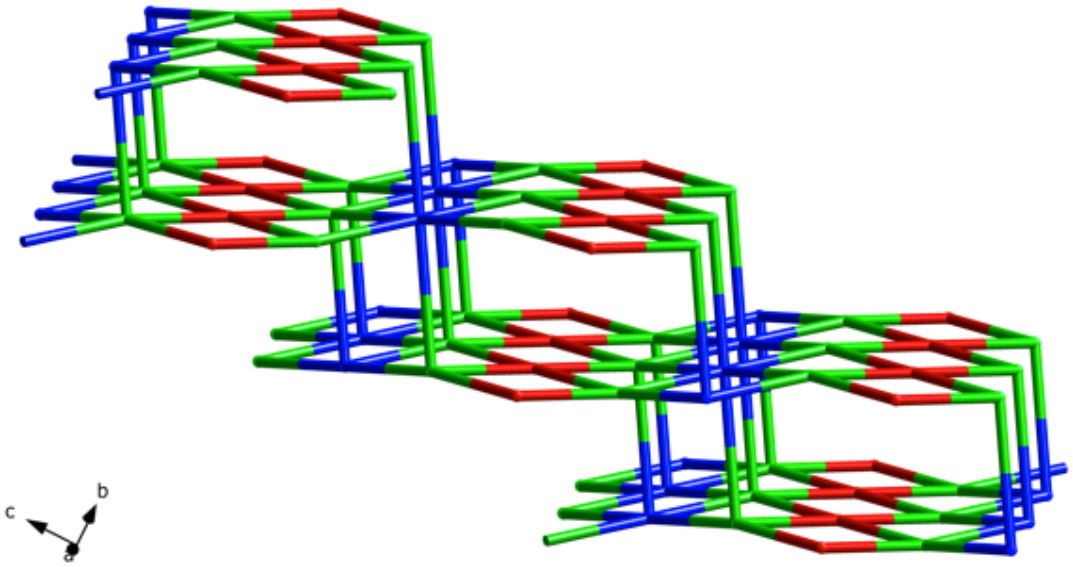

Figure 10